Phylogeography of Noah's giant clam

Cécile Fauvelot, Serge Andréfouët, Daphné Grulois, Josina Tiavouane, Colette C C Wabnitz, Hélène Magalon, Philippe Borsa

To be cited as: Fauvelot C, Andréfouët S, Grulois D, Tiavouane J, Wabnitz CCC, Magalon H, Borsa P (2019) Phylogeography of Noah's giant clam. Marine Biodiversity 49, 521–526. doi : 10.1007/s12526-017-0794-0

Phylogeography of Noah's giant clam

Cécile Fauvelot[1,2*], Serge Andréfouët[1], Daphné Grulois[1], Josina Tiavouane[1], Colette C C Wabnitz[3,4], Hélène Magalon[5], Philippe Borsa[1]

[1] UMR ENTROPIE (IRD, Université de La Réunion, CNRS), Laboratoire d'excellence CORAIL; centre IRD de Nouméa, New Caledonia
[2] Present address: Université Côte d'Azur, CNRS, FRE 3729 ECOMERS, Parc Valrose, Nice, France
[3] Secretariat of the Pacific Community, Nouméa, New Caledonia
[4] Present address: Changing Ocean Research Unit, Institute for the Oceans and Fisheries, University of British Columbia. Aquatic Ecosystems Research Lab. Vancouver, BC V6T 1Z4. Canada
[5] UMR ENTROPIE (Université de La Réunion, CNRS, IRD), Laboratoire d'excellence CORAIL; Université de La Réunion, St Denis, La Réunion
*Corresponding author: cecile.fauvelot@ird.fr

Abstract Noah's giant clam (*Tridacna noae*), recently resurrected from synonymy with *T. maxima*, occurs from Christmas Island to the Northern Line Islands and from the Ryukyu Islands to New Caledonia. We used mitochondrial and microsatellite markers to investigate the phylogeographic structure and demographic history of *T. noae* over most of its geographical range. Results from the two types of markers reveal a consistent population structure, partitioning *T. noae* into three distinct lineages: (1) eastern half of the Indo-Malay archipelago and Western Australia, (2) Melanesia and Micronesia, and (3) Central Polynesia. Demographic expansion initiated between 300,000 and 400,000 years ago was detected for each haplogroup. This pattern, which is congruent with other co-occurring *Tridacna* species, indicates a shared evolutionary history with expansion from past refuges following late-Pleistocene sea-level changes.

Keywords: *Tridacna*, evolutionary history, mitochondrial DNA, microsatellite, Indo-Pacific

Introduction

Phylogeographic studies of endangered giant clams [Hui et al. (2016) and references therein] have revealed complex patterns, shedding new light on their ecology and evolution and providing important information to assist in their conservation. Because of previous confusion of the recently resurrected Noah's giant clam *Tridacna noae* with the small giant clam *T. maxima* (Huelsken et al. 2013; Su et al. 2014; Johnson et al. 2016), little is known of its phylogeographic structure. *Tridacna noae* presents a large distribution, from the Ryukyu Islands southward to Western Australia and New Caledonia, and from Christmas Island (Indian Ocean) eastward to Kiritimati in the northern Line Islands (Borsa et al. 2015; Neo and Low 2017). Substantial genetic differences have been reported between *T. noae* populations from Ningaloo Reef and the Solomon Islands, mostly similar to the phylogeographic patterns uncovered for *T. crocea* and *T. maxima* (Huelsken et al. 2013). Expanding on previous research, here we examine the phylogeographic structure of *T. noae* over most of its geographic range using mitochondrial and microsatellite markers, and infer past demographic changes for this species.

Materials and methods

Mantle biopsies of a total of 87 *Tridacna noae* individuals were collected from nine localities in the Indo-West Pacific (Fig. 1a, Table 1). Genomic DNA was extracted using the DNeasy Blood and Tissue kit (Qiagen,Valencia CA). The 5'-end fragment of the mitochondrial cytochrome *c* oxidase subunit I gene (*COI*) was amplified using primers *CO1-Tricro-F* and *CO1-Tricro-R* (Kochzius and Nuryanto 2008) or *TF1* and *RF1* (Lizano and Santos 2014), with the annealing temperature set to 48°C. Polymerase-chain reaction products were sent to GATC Biotech (Konstanz) for sequencing on an ABI 3730XL Genetic Analyzer (Applied Biosystems, Carlsbad CA), using the forward primer. We also analyzed allele size variation at 15 microsatellite loci specifically developed for *T. maxima* (Grulois et al. 2015). Amplification reactions and allele sizing were done as in Grulois et al. (2015).

Eighty *COI* gene sequences were obtained and aligned along 18 previously published sequences (Table 1) under BIOEDIT v. 7.1.3.0 (Hall 1999). The resulting sequence matrix was trimmed to 364 base pairs starting at the nucleotide site homologous to site 222 of the *COI* gene of *Acanthocardia tuberculata* (Cardiidae) (GenBank DQ632743; Dreyer and Steiner 2006). A median-joining parsimony network was constructed under NETWORK v. 4.6.1.3 using default settings (Bandelt et al. 1999). Mean net nucleotide divergences among haplogroups (see Results) were estimated based on the T92+G nucleotide substitution model (Tamura 1992); $G = 0.19$), selected according to the Bayesian information criterion in MEGA4 (Tamura et al. 2007). Genetic differentiation among populations was estimated by Φ_{ST} based on the T92+G model in a hierarchical analysis of molecular variance (AMOVA) under ARLEQUIN v. 3.5 (Excoffier and Lischer 2010), where populations were grouped into three major geographic regions consistent with mitochondrial haplogroup structure (Fig. 1b). Departures from the selective neutrality and population equilibrium were further tested within each haplogroup with Tajima's *D* (Tajima 1989) and Fu's *Fs* tests (Fu 1997) using ARLEQUIN. Pairwise mismatch distributions (Rogers and Harpending 1992) within each haplogroup were compared to those expected under Rogers' (1995) model of sudden population expansion and Excoffier's (2004) model of spatial expansion (Excoffier and Lischer 2010) using ARLEQUIN. Time to the most recent

common ancestor (TMRCA) for each haplogroup was estimated from an ultrametric tree calibrated with fossil data (all details given in Online Resource 1) under BEAST v. 1.8.3 (Drummond et al. 2012). The TMRCA estimates were then used as node priors for each haplogroup under the constant-size Bayesian skyline plot model in BEAST (10^7 Markov-chain Monte Carlo generations, sampled every 10^3 generations and using the same parameters as for the phylogenetic analysis). TRACER v. 1.5 (Rambaut et al. 2014) was used to determine convergence and to plot demographic skylines. The null hypothesis of constant population size was rejected when the lower bound of the 95% high posterior density (HPD) of this distribution was higher than zero. The beginning of the population expansion was identified from the skyline output as the point when the effective population size started to increase.

From the 15 microsatellite markers initially developed for *T. maxima*, six that cross-amplified with *T. noae* were retained for routine scoring. Due to low sample sizes, some samples from adjacent localities and for which mtDNA haplotypes belonged to the same haplogroup (see Results) were pooled: Kosrae with Tarawa, and Upolu with Wallis. Genetic diversity (H_E) was estimated with GENETIX v. 4.05 (Belkhir et al. 2004) and compared to the observed value (H_O). Deviations from Hardy-Weinberg equilibrium (HWE) were estimated using Weir and Cockerham's (1984) inbreeding coefficient (*f*), and assessed using exact tests in GENEPOP v. 4.2 (Raymond and Rousset 1995). Null-allele frequencies were estimated using Dempster et al.'s (1977) EM algorithm in FREENA (Chapuis and Estoup 2007). Genetic differentiation among populations [Weir's (1996) F_{ST}] was estimated using FREENA with correction for null alleles (ENA method; Chapuis and Estoup 2007). Correlations between pairwise F_{ST} (or Φ_{ST}) and geographic distance were tested using Mantel's test (10^4 permutations; GENETIX).

Results and discussion

Significant single-locus deviations from genotype frequencies expected under HWE were observed in three populations of *Tridacna noae* and for one or two microsatellite loci (table given in Online Resource 2). Overall, these deviations were ascribed to null alleles occurring at four loci. Null alleles may be caused by mis-priming, an expected outcome given that the microsatellite primers were designed for *T. maxima*, which is separated from *T. noae* by substantial nucleotide divergence (17%-24%) at the *COI* locus (Borsa et al. 2015). Corrected pairwise F_{ST} estimates ranged from 0.016 (P = 0.054) between the Bismarck Sea and (Kosrae + Tarawa), to 0.082 ($P < 0.001$) between Taiwan and (Wallis + Upolu), revealing strong and significant genetic structure across the geographic range of *T. noae* (Table 2). Noteworthy, these pairwise F_{ST} estimates were highly correlated (R^2= 0.792, $P <$ 0.0001) with pairwise F_{ST} estimated using the two microsatellite loci in HWE (*TmB12* and *Tm25349*), suggesting that null alleles have little influence on corrected F_{ST} estimates. Only five out of the 15 pairwise comparisons were not significant, resulting in four partially overlapping groups (Fig. 1a: inset). Only (Wallis + Upolu) was significantly distinct from all other populations (Table 2). No correlation (R^2 = 0.168, P = 0.180) was found between genetic and geographic distances (see Online Resource 3).

Mitochondrial haplotypes clustered into three distinct haplogroups (Fig. 1b, inset), each specific to a particular geographic region. The net nucleotide divergence (mean ± standard error) was 0.029 ± 0.011 between Haplogroups I and II, 0.050 ± 0.015 between Haplogroups II and III, and 0.059 ±

0.019 between Haplogroups I and III. These values were 2.4 to 11.1 times less than inter-specific estimates of nucleotide divergence in *Tridacna* spp. (0.139 to 0.322; Borsa et al. 2015), but the present results still suggest relatively deep inter-lineage differentiation, comparable to the inter-lineage differences in *T. crocea*, *T. maxima* and *T. squamosa* (DeBoer et al. 2014). Variable levels of genetic differentiation were observed among populations, with Φ_{ST} estimates ranging from nearly 0 between sites within a region to 0.973 between the two most distant sites (Taiwan and Upolu) (Table 2). A large proportion of the molecular variance (45%; $P = 0.022$) was found among regions (Fig. 1b). Weak correlation was observed between $\Phi_{ST}/(1- \Phi_{ST})$ and geographic distance ($P = 0.048$; see Online Resource 3). Tajima's (1989) *D* was negative and significant in all three haplogroups (-1.65 to -1.15; Fisher's combined $P < 0.01$), as was Fu's (1997) *Fs* (-34.03 to -26.76; $P < 0.001$). Although Rogers's (1995) sudden expansion model was rejected ($P < 0.006$ for all three mitochondrial haplogroups), Excoffier's (2004) spatial expansion model was not ($P > 0.131$). Significant demographic expansion was detected for each haplogroup (Bayesian skyline plots: Fig. 2a-c). Skyline outputs suggest that expansion was initiated ca. 400,000 years ago for Haplogroups I and II, and ca. 300,000 years ago for Haplogroup III.

The present findings illustrate that the genetic divergence previously observed between *T. noae* from Ningaloo Reef and the Solomon Islands (Huelsken et al. 2013) reflects distinct lineages, and not isolation by distance. Mitochondrial markers assigned the Ningaloo population to Haplogroup I and the Solomon population to the distinct Haplogroup II. The latter characterizes populations from Melanesia and Micronesia (Lineage 2; Fig. 1a). This phylogeographic discontinuity between the Indo-Malay-Australia region and Melanesia seems to coincide with the phylogeographic break observed across three other co-distributed *Tridacna* species (Gardner et al. 2012; Huelsken et al. 2013; DeBoer et al. 2014; Hui et al. 2016). The consistency between mitochondrial and nuclear markers indicates that phylogeographic structure is a result of long-lasting differentiation. The co-occurrence of Haplogroups I and II in Yap and non-significant differentiation between Taiwan and Yap based on the nuclear markers both point to secondary contact. A more in-depth analysis of the genetic structure of *T. noae* around Yap and neighbouring islands (Chuuk, Palau and Guam, for example) would help map the zone of overlap in this region, which is recognized as a dispersal corridor between the Coral Triangle and the central Pacific (Davies et al. 2015), and assess the degree of reproductive isolation between lineages.

Evidence of spatial expansion was compatible with negative Tajima's (1989) *D* values and large negative *Fs* values (Fu 1997), and supported by the demographic history inferred from both the mitochondrial DNA coalescent simulation analysis and the Bayesian skyline plots. The estimated timings of expansion initiation for the different haplogroups are in the range of recently published estimates for Indo-Pacific reef-associated organisms (Ludt et al. 2012; Delrieu-Trottin et al. 2017). The observed differences in the onset of the expansion among haplogroups suggest a more recent expansion of the Polynesian lineage. This finding is in agreement with the theory that older populations are more likely to be closer to the center of the Coral Triangle than to peripheral locations (Evans et al. 2016). Deep phylogeographic structure combined with evidence of spatial expansion points to an allopatric scenario, where ancestral populations in the late Pleistocene were confined to refuges (Pellissier et al. 2014).

In conclusion, the relative consistency of phylogeographic structure across four *Tridacna* species (*T. crocea*, *T. maxima*, *T. squamosa* and now *T. noae*) suggests a shared history of geographic isolation.

During low sea-level periods, the distribution of shallow-water reef habitats favorable to giant clams was profoundly affected (Lambeck and Chappell 2001) and viable populations of a number of Indo-Pacific reef-associated organisms survived in refuges that were isolated from each other (Pellissier et al. 2014). Once sea levels rose again, surviving populations, by then forming differentiated lineages, re-expanded to reach their current geographic distributions.

Acknowledgments We thank P. Bosserelle (Wallis), J. Butscher (New Caledonia), P. Dor (Yap), C. Payri (Madang), M. Sapatu (Samoa), M. Savins (Kiribati), M. Selch (Kosrae) and B.-W. Su (Dongsha) for assistance in obtaining giant clam biopsies. Sampling in New Caledonia was carried out during the BIBELOT cruise (doi:http://dx.doi.org/10.17600/13100100). Local communities, Ian Bertram (SPC) and staff from fisheries offices and relevant government institutions in SPC member countries are acknowledged for their kind support and cooperation in obtaining samples and required permits. Sample collection and/or shipment was in part facilitated by a grant from the Australian government (DFAT) to SPC's FAME division. Genetic analyses were co-funded by the BeN-Co project (ZoNéCo program, New Caledonia) and the TriMax project (Laboratoire d'excellence CORAIL, Agence nationale de la recherche, France).This is ENTROPIE contribution #181.

References

Bandelt HJ, Forster P, Röhl A (1999) Median-joining networks for inferring intraspecific phylogenies. Mol Biol Evol 16:37-48.

Belkhir K, Borsa P, Chikhi L, Raufaste N, Bonhomme F (2004) GENETIX 4.05, logiciel sous Windows™ pour la génétique des populations. Laboratoire Génome, Populations, Interactions, CNRS UMR 5000, Université Montpellier II, Montpellier.

Borsa P, Fauvelot C, Tiavouane J, Grulois D, Wabnitz CCC, Abdon Naguit MR, Andréfouët S (2015) Distribution of Noah's giant clam, *Tridacna noae*. Mar Biodiv 45:339–344., doi: 10.1007/s12526-014-0265-9

Chapuis MP, Estoup A (2007) Microsatellite null alleles and estimation of population differentiation. Mol Biol Evol 24:621–31., doi: 10.1093/molbev/msl191

Davies SW, Treml EA, Kenkel CD, Matz MV (2015) Exploring the role of Micronesian islands in the maintenance of coral genetic diversity in the Pacific Ocean. Mol Ecol 24:70–82., doi: 10.1111/mec.13005

DeBoer TS, Abdon Naguit MR, Erdmann MV, Ablan-Lagman MCA, Ambariyanto, Carpenter KE, Toha AHA, Barber PH (2014) Concordance between phylogeographic and biogeographic boundaries in the Coral Triangle: conservation implications based on comparative analyses of multiple giant clam species. Bull Mar Sci 90:277–300., doi: 10.5343/bms.2013.1003

Delrieu-Trottin E, Mona S, Maynard J, Neglia V, Veuille M, Planes S (2017) Population expansions dominate demographic histories of endemic and widespread Pacific reef fishes. Sci Rep 7:40519., doi: 10.1038/srep40519

Dempster AP, Laird NM, Rubin DB (1977) Maximum likelihood from incomplete data via the EM algorithm. J R Stat Soc Ser B 39:1–38.

Dreyer H, Steiner G (2006) The complete sequences and gene organisation of the mitochondrial genomes of the heterodont bivalves *Acanthocardia tuberculata* and *Hiatella arctica* – and the first record for a putative Atpase subunit 8 gene in marine bivalves. Front Zool 3:13., doi: 10.1186/1742-9994-3-13

Drummond AJ, Suchard MA, Xie D, Rambaut A (2012) Bayesian phylogenetics with BEAUti and the BEAST 1.7. Mol Biol Evol 29:1969–1973., doi: 10.1093/molbev/mss075

Evans SM, McKenna C, Simpson SD, Tournois J, Genner MJ (2016) Patterns of species range evolution in Indo-Pacific reef assemblages reveal the Coral Triangle as a net source of transoceanic diversity. Biol Lett 12:20160090., doi: 10.1098/rsbl.2016.0090

Excoffier L (2004) Patterns of DNA sequence diversity and genetic structure after a range expansion: lessons from the infinite-island model. Mol Ecol 13:853–864., doi: 10.1046/j.1365-294X.2003.02004.x

Excoffier L, Lischer HEL (2010) Arlequin suite ver 3.5: a new series of programs to perform population genetics analyses under Linux and Windows. Mol Ecol Resour 10:564–567., doi: 10.1111/j.1755-0998.2010.02847.x

Fu YX (1997) Statistical tests of neutrality of mutations against population growth, hitchhiking and background selection. Genetics 147:915–925.

Gardner JPA, Boesche C, Meyer JM, Wood AR (2012) Analyses of DNA obtained from shells and brine-preserved meat of the giant clam *Tridacna maxima* from the central Pacific Ocean. Mar Ecol ProgSer 453:297–301., doi: 10.3354/meps09625

Grulois D, Tiavouane J, Dumas PP, Fauvelot C (2015) Isolation and characterization of fifteen microsatellite loci for the giant clam *Tridacna maxima*. Conserv Genet Resour 7:73–75., doi: 10.1007/s12686-014-0290-9

Hall T.A. (1999) BioEdit: A user-friendly biological sequence alignment editor and analysis program for Windows 95/98/NT. Nucleic Acids Symp Ser 41:95–98.

Huelsken T, Keyse J, Liggins L, Penny S, Treml EA, Riginos C (2013) A novel widespread cryptic species and phylogeographic patterns within several giant clam species (Cardiidae: *Tridacna*) from the Indo-Pacific Ocean. PLoS One 8:e80858., doi: 10.1371/journal.pone.0080858

Hui M, Kraemer WE, Seidel C, Nuryanto A, Joshi A, Kochzius M (2016) Comparative genetic population structure of three endangered giant clams (Cardiidae: *Tridacna* species) throughout the Indo-West Pacific: implications for divergence, connectivity and conservation. J Mollus Stud 82:403–414., doi: 10.1093/mollus/eyw001

Johnson MS, Prince J, Brearley A, Rosser NL, Black R (2016) Is *Tridacna maxima* (Bivalvia: Tridacnidae) at Ningaloo Reef, Western Australia? Mollus Res 1–7., doi: 10.1080/13235818.2016.1181141

Kochzius M, Nuryanto A (2008) Strong genetic population structure in the boring giant clam, *Tridacna crocea*, across the Indo-Malay archipelago: implications related to evolutionary processes and connectivity. Mol Ecol 17:3775–87., doi: 10.1111/j.1365-294X.2008.03803.x

Lambeck K, Chappell J (2001) Sea level change through the last glacial cycle. Science 292:679–686., doi: 10.1126/science.1059549

Lizano AMD, Santos MD (2014) Updates on the status of giant clams *Tridacna* spp. and *Hippopushippopus* in the Philippines using mitochondrial *CO1* and *16S rRNA* genes. Philipp Sci Lett 7:187–200.

Ludt WB, Bernal MA, Bowen BW, Rocha LA (2012) Living in the Past: Phylogeography and population histories of Indo-Pacific wrasses (Genus *Halichoeres*) in shallow lagoons versus outer reef slopes. PLoS One., doi: 10.1371/journal.pone.0038042

Neo ML, Low JKY (2017) First observations of *Tridacna noae* (Röding, 1798) (Bivalvia: Heterodonta: Cardiidae) in Christmas Island (Indian Ocean). Mar Biodiv., doi: 10.1007/s12526-017-0678-3

Pellissier L, Leprieur F, Parravicini V, Cowman PF, Kulbicki M, Litsios G, Olsen SM, Wisz MS, Bellwood DR, Mouillot D (2014) Quaternary coral reef refugia preserved fish diversity. Science 344:1016–1019., doi: 10.1126/science.1249853

Rogers A (1995) Genetic evidence for a Pleistocene population explosion. Evolution 49:608-615.

Rogers AR, Harpending H (1992) Population growth makes waves in the distribution of pairwise genetic differences. Mol Biol Evol 9:552–569.

Su Y, Hung JH, Kubo H, Liu LL (2014) *Tridacna noae* (Röding, 1798) – a valid giant clam species separated from *T. maxima* (Röding, 1798) by morphological and genetic data. Raffles Bull Zool 62:124–135.

Tajima F (1989) Statistical method for testing the neutral mutation hypothesis by DNA polymorphism. Genetics 123:585–595.

Tamura K (1992) Estimation of the number of nucleotide substitutions when there are strong transition-transversion and G+C-content biases. Mol Biol Evol 9:678–687.

Tamura K, Dudley J, Nei M, Kumar S (2007) MEGA4: Molecular Evolutionary Genetics Analysis (MEGA) software version 4.0. Mol Biol Evol 24:1596–9., doi: 10.1093/molbev/msm092

Weir BS, Cockerham CC (1984) Estimating *F*-statistics for the analysis of population structure. Evolution 38:1358–1370., doi: 10.2307/2408641

Table 1 *Tridacna noae* sampling details and GenBank accession numbers for *COI* gene sequences. List of sampling locations arranged from west to east. *N:* sample size. In brackets: number of *COI* sequences. *NA*: not available

Location	Abbrev-iation	Year	*N*		GenBank no.	Reference
Ningaloo Reef, Western Australia	NR	NA	6	(6)	JX974903- JX974908	Huelsken et al. (2013)
Dongsha Island, South China Sea	Tai.	2013	10	(9)	KT899615- KT899623	present study
Taiwan	Tai.	2005-08	2	(2)	DQ168140, KC456023	Su et al. (2014)
Sibulan, Negros Island, Philippines	NI	NA	3	(3)	KJ20211416	Lizano & Santos (2014)
Doi Island, Molucca Sea	MS	NA	1	(1)	KF446463	DeBoer et al. (2014a)
Yap, Fed. States of Micronesia	Yap	2014	8	(8)	KT899644- KT899651	present study
Madang, Bismarck Sea	BS	2013	1	(1)	KT899681	present study
Kavieng, Bismarck Sea	BS	2014	17	17)	KT899624- KT899640	present study
Solomon Islands	Sol.	NA	6	(6)	JX974918-23	Huelsken et al. (2013)
Kosrae, Fed. States of Micronesia	Kos.	2014	4	(4)	KT899652- KT899655	present study
Loyalty Islands, New Caledonia	NC	2014	14	13)	KT899682- KT899694	present study
Tarawa, Gilbert Islands, Kiribati	Tar.	2014	1	(1)	KT899680	present study
Wallis Island, Wallis and Futuna	Wal.	2014	3	(3)	KT899641- KT899643	present study
Upolu, Western Samoa	Upo.	2014	29	24)	KT899656- KT899679	present study

Table 2 Genetic differentiation among *Tridacna noae* populations. *Above diagonal* (in grey): population-pairwise Φ_{ST} estimates based on partial *COI* gene sequences. *Below diagonal*: population-pairwise F_{ST} estimates based on six microsatellite loci. *Tai.* Taiwan; *NI* Negros Island, Philippines; *MS* Doi Island, Molucca Sea; *NR* Ningaloo Reef, Western Australia; *BS* Bismark Sea, Papua New Guinea; *Sol.* Solomon Islands; *Kos.* Kosrae, Federal State of Micronesia; *NC* New Caledonia; *Tar.* Tarawa, Gilbert Islands, Kiribati; *Wal.* Wallis; *Upo.* Upolu, Western Samoa

Sample	Sample									
	Tai.	Yap	NI+MS	NR	BS	Kos+Tar	NC	Sol.	Wal.	Upo.
Tai.		0.652**	0.821**	0.839**	0.884**	0.951**	0.842**	0.898**	0.960**	0.973**
Yap	0.046		0.001	0.627**	0.736**	0.746**	0.661**	0.695**	0.862**	0.941**
NI+MS	-	-		0.824**	0.814**	0.937**	0.734**	0.816**	0.947*	0.973**
NR	-	-	-		0.874**	0.948**	0.819**	0.878**	0.955*	0.976**
BS	0.080**	0.032	-	-		0.298*	0.019	0.001	0.879**	0.927**
Kos.+Tar.	0.065**	0.042	-	-	0.016		0.121	0.205	0.946**	0.968**
NC	0.044**	0.071**	-	-	0.048**	0.035		0.001	0.819**	0.908**
Sol.	-	-	-	-	-	-	-		0.866**	0.947**
Wal. + Upo.	0.082**	0.072**	-	-	0.056**	0.044*	0.018**	-		0.034

* $P < 0.05$; **$P < 0.01$ [at the mitochondrial locus: the significance of Φ_{ST} and associated variance components were tested by 10^4 random permutations under ARLEQUIN(Excoffier and Lischer 2010). At microsatellite loci: the genotypic differentiation was tested using Fisher's exact test implemented in GENEPOP (Raymond & Rousset 1995)].

Figure captions

Fig. 1 Sampling locations for *Tridacna noae*. *Stars*: samples from previous studies (Huelsken et al. 2013; DeBoer et al. 2014; Lizano and Santos 2014; Su et al. 2014); *solid circles*: new samples (present study). *Abbreviations for samples* as in Table 1. **(a)** Geographic distribution of lineages as defined by allele frequencies at six microsatellite loci. *Inset*: Multi-dimensional scaling plot [*cmdscale* function in R v. 3.1.0 (www.r-project.org/)] of samples based on standardized pairwise F_{ST} [$F_{ST}/(1-F_{ST})$] estimated from allele-frequencies at six microsatellite loci, with correction for null alleles. *Polygons* delineate groups of samples for which pairwise F_{ST} values were not significant (Table 2). *Long-dash line*: Lineage 1; *short-dash line*: Lineage 2; *solid line*: Lineage 3; *dotted line*: Lineage 4. **(b)** Geographic distribution of mitochondrial haplogroups. *Long-dashline*: Haplogroup I; *short-dashline*: Haplogroup II; *dotted line*: Haplogroup III. *Inset*: Median-Joining parsimony network of 98 *COI* gene sequences. *Grey tones* distinguish geographic regions: *light-grey*: haplotypes from the central Indo-West Pacific (Ningaloo Reef, Dongsha Island, Taiwan, Negros Island, Molucca Sea, Yap); *white*: haplotypes from the western Pacific (Yap, Bismarck Sea, Solomon Islands, Kosrae, New Caledonia, Tarawa); *black*: haplotypes from Central Polynesia (Wallis, Upolu). *Scale bar*: 1 mutation step; *numbers* count mutations between two adjacent haplogroups; *circle surface* proportional to number of sequences.

Fig. 2 Demographic history of *Tridacna noae* over the last one million years. Bayesian skyline plot reconstructions for each of the three *T. noae* mitochondrial haplogroups (see Fig. 1b). The skyline plot of each haplogroup was time-calibrated using the mean date assigned to the last common ancestor (posterior mean indicated as vertical dotted line), estimated from a fossil-calibrated phylogeny according to the Yule model of speciation (see Online Resource 1 for details). The dashed lines delineate the interval that contains 95% of the probability of the posterior distribution (95% HPD) and the thick line is the median. *Ne* effective population size of females; τ generation time (in My). (**a**) Haplogroup I. (**b**) Haplogroup II. (**c**) Haplogroup III.

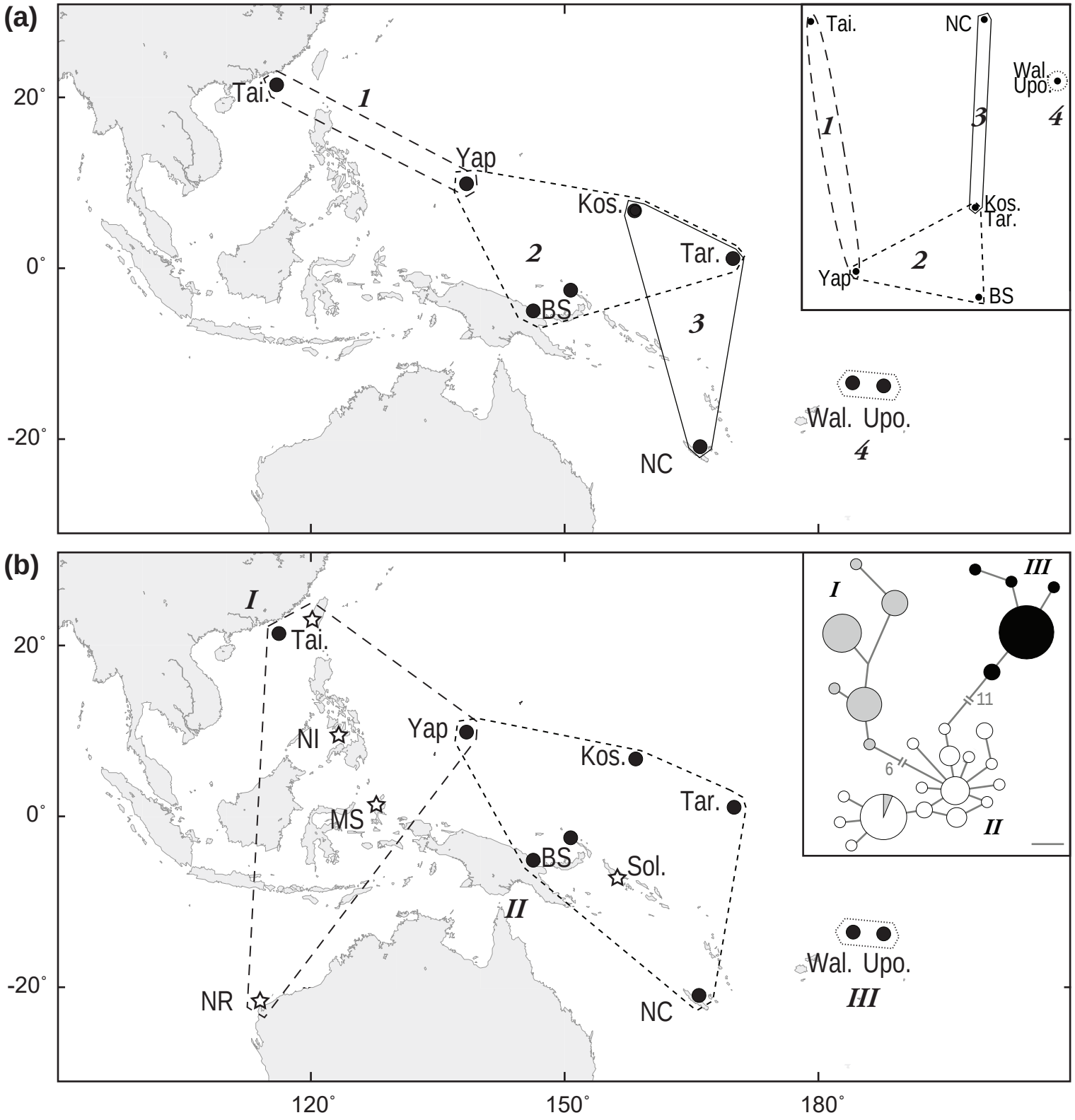
(a)
20˚
0˚
-20˚
Tai.
Yap
Kos.
Tar.
BS
NC
Wal. Upo.
1
2
3
4
(b)
I
II
III
NI
MS
NR
Sol.
120˚
150˚
180˚
11
6

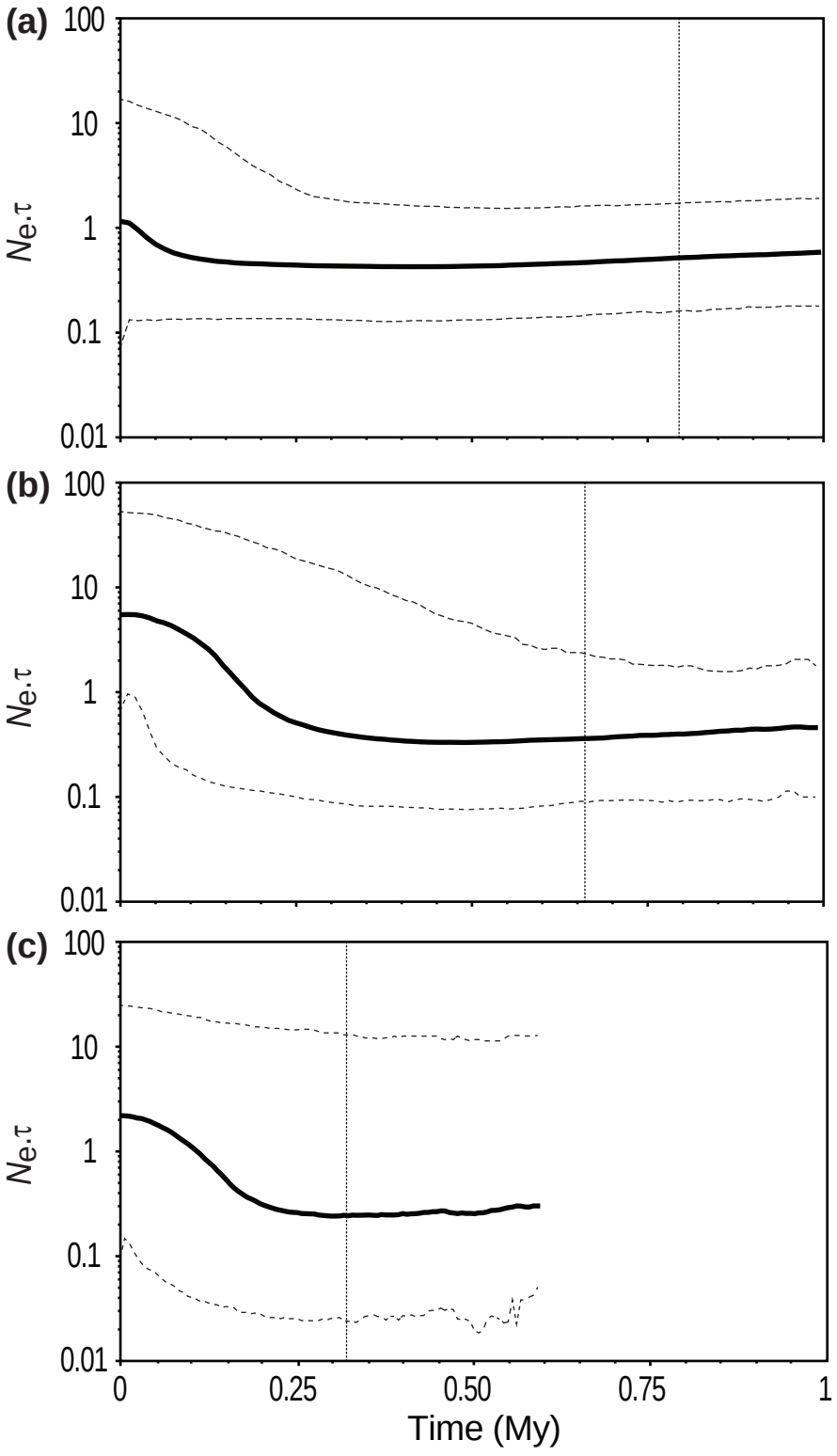
(a)
(b)
(c)
100
10
1
0.1
0.01
$N_{e.\tau}$
0
0.25
0.50
0.75
1
Time (My)

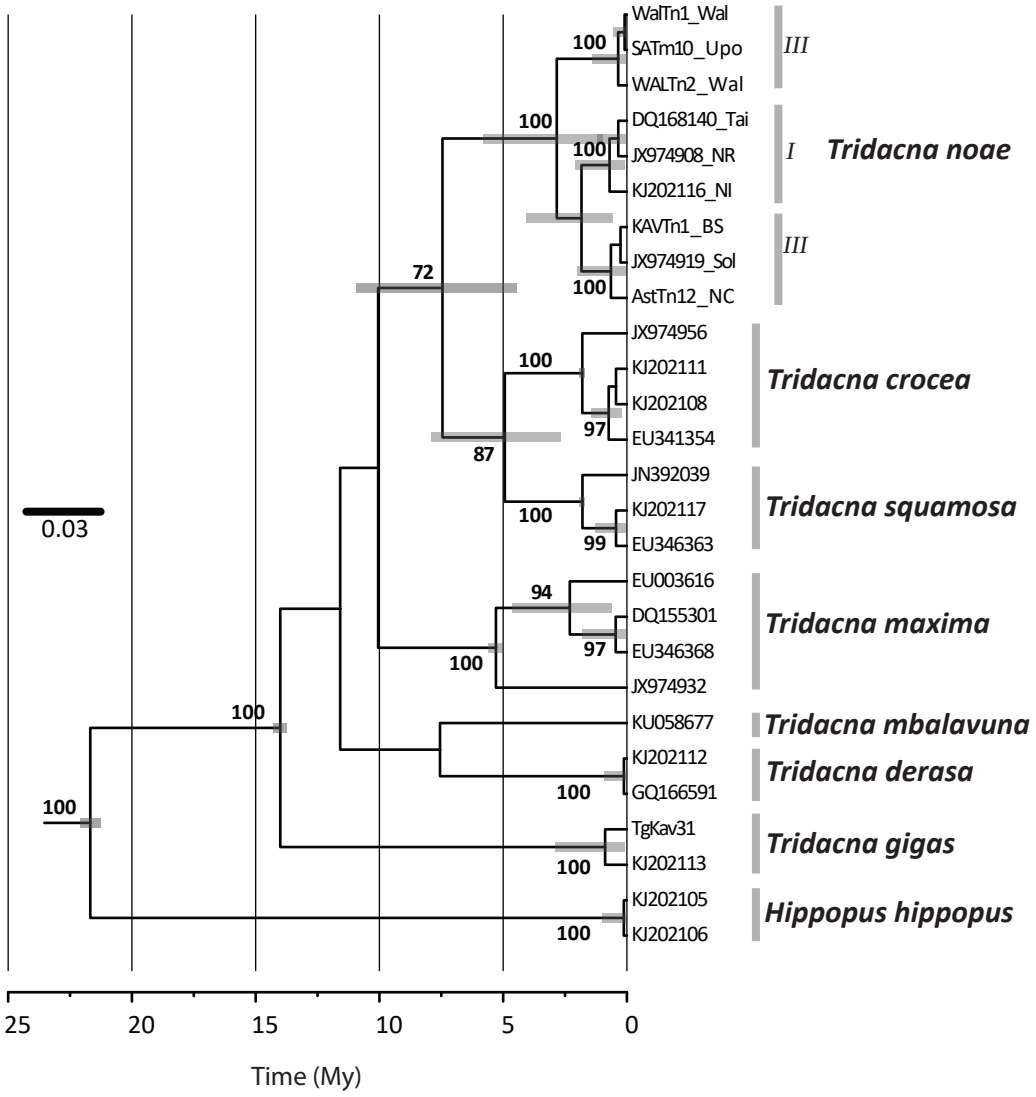

Online Resource 1 Time-calibrated maximum clade credibility tree of Tridacninae (including species in the genera *Hippopus* and *Tridacna*) based on partial mitochondrial COI gene sequences. The tree was constructed using BEAST v. 1.8.3 (Drummond et al. 2012) using a Yule model of speciation. This tree was rooted with the homologous sequence from *Acanthocardia tuberculata* (GenBank DQ632743). Time [in millions of years (My)] is represented at the bottom of the tree. Posterior mean nodal ages with 95% highest posterior density (HPD) intervals are indicated by horizontal grey bars. Estimated time to most recent common ancestor were 0.08-2.09 My (mean 0.87 My) for *T. noae* Haplogroup I, 0.05-1.98 My (mean 0.81 My) for Haplogroup II, and 0.01-1.40 My (mean 0.50 My) for Haplogroup III. *Scale bar*: 3 % genetic divergence. Bayesian posterior probabilities of nodes estimated by BEAST are indicated when > 70%. Up to four individuals per giant clam species (or haplogroup in *T. noae*) were retained for the analysis. Nucleotide sequences were either from present study, or downloaded from GenBank (http://ncbi.nlm.nih.gov/). Sequences were aligned under BIOEDIT v.7.1.3.0 (Hall 1999), and trimmed to a common length of 364 bp. The HKY model (Hasegawa et al.1985) with gamma-distributed substitution rates and invariant sites (+G+I) was selected, with partitioning by codon position (1+2, 3). A relaxed molecular clock with an uncorrelated lognormal mutation rate was used. We applied a lognormal prior distribution to all fossil calibrations, with the means and standard deviations of the distributions set to represent the 95% estimated confidence interval for the origination of a taxon based on its first occurrence in the fossil record. Node calibrations were based on Schneider and O'Foighil (1999), Harzhauser et al. (2008), Jablonski et al. (2013), and Herrera et al. (2015). Priors for mean of nodal ages were 21.7 My for Tridacninae [initial = 20.3 My, log(StDev) = 0.01]; 14 My for the genus Tridacna [initial = 13.8 My, log(StDev) = 0.01]; 5.3 My for *T. maxima* [initial = 5.0 My, log(StDev)=0.03]; 1.8 My for *T. crocea* and *T. squamosa* [initial = 1.5 My, log(StDev)=0.03]. Speciation was modeled under a Yule process through 3 independent runs of 50 million Markov-Chain Monte Carlo generations, recorded every 1000th generation, with a 10% burn-in. The three runs were combined using LogCombiner and TreeAnnotator v.1.8.3 and the consensus tree was visualized in FigTree v.1.4.2

Drummond AJ, Suchard MA, Xie D, Rambaut A (2012) Bayesian phylogenetics with BEAUTI and the BEAST 1.7. Mol Biol Evol 29:1969–1973

Hall TA (1999) BIOEDIT: a user-friendly biological sequence alignment editor and analysis program for Windows 95/98/NT. Nucl Acids Symp Ser 41:95-98

Harzhauser M, Mandic O, Piller WE, Reuter M, Kroh A (2008) Tracing back the origin of the Indo-Pacific mollusc fauna: Basal Tridacninae from the Oligocene and Miocene of the Sultanate of Oman. Palaeontology 51:199–213

Hasegawa M, Kishino H, Yano T (1985) Dating of human-ape splitting by a molecular clock of mitochondrial DNA. J Mol Evol 22:160-174

Herrera ND, ter Poorten JJ, Bieler R, Mikkelsen PM, Strong EE, Jablonski D, Steppan SJ (2015) Molecular phylogenetics and historical biogeography amid shifting continents in the cockles and giant clams (Bivalvia: Cardiidae). Mol Phylogenet Evol 93:94-106

Jablonski D, Belanger CL, Berke SK, Huang S, Krug AZ, Roy K, Tomasovych A, Valentine JW (2013) Out of the tropics, but how? Fossils, bridge species, and thermal ranges in the dynamics of the marine latitudinal diversity gradient. Proc Natl Acad Sci USA 110:10487-10494

Schneider JA, O'Foighil D (1999) Phylogeny of giant clams (Cardiidae:Tridacninae) based on partial mitochondrial 16S rDNA gene sequences. Mol Phylogenet Evol 13:59-66

Online Resource 2 Summary of genetic diversity at six microsatellite loci for *Tridacna noae* samples; *N* sample size; H_0 observed heterozygosity; H_E Nei 's (1987) genetic diversity (unbiased); *f* Weir and Cockerham's (1984) fixation index. *Asterisks* indicate significant deviations from Hardy-Weinberg equilibrium ($P < 0.0013$ after Bonferroni adjustment). *NA* estimated null allele frequency. See Table 1 for sample abbreviations

Locus, Parameter	Sample (*N*)					
	Tai. (10)	Yap (8)	BS (18)	Kos.+Tar. (5)	NC (14)	Wal.+Upo. (32)
Tm24162						
H_E	0.857	0.687	0.908	0.880	0.888	0.879
H_O	0.571	0.750	0.941	1	0.909	0.687
f	0.400	0.053	-0.006	-0.026	0.024	0.248
NA	0.439	0.556	0.070	0	0.414	0.574
Tm25349						
H_E	0.376	0.117	0.0540	0	0	0
H_O	0.444	0.125	0.0556	0	0	0
f	-0.123	0	0	-	-	-
NA	0.200	0	0	0.001	0.577	0.177
Tm6526						
H_E	0.679	0	0.825	0.500	0.812	0.722
H_O	0.125	0	0.765	0	0.500	0.333
f	0.837*	-	0.103	1	0.500*	0.667
NA	0.502	0.791	0.124	0.787	0.832	0.937
TmB12						
H_E	0.759	0.781	0.874	0.820	0.862	0.821
H_O	0.778	0.750	0.889	0.600	0.928	0.812
f	0.034	0.106	0.011	0.368*	-0.040	0.026
NA	0.159	0.010	0	0.105	0	0
TmE4						
H_E	0.720	-	0	-	0.660	0.734
H_O	0.400	-	0	-	0.200	0.500
f	0.529	-	-	-	0.750*	0.378
NA	0.640	1	0.782	1	0.830	0.811
TmE5						
H_E	0.750	0.444	0.667	0	0.500	0.819
H_O	0.667	0	0	0	0	0.666
f	0.200	1	1	-	1	0.273
NA	0.486	0.800	0.915	0.894	0.944	0.843
Multilocus						
H_E	0.690	0.406	0.555	0.440	0.619	0.663
H_O	0.498	0.325	0.442	0.320	0.426	0.500
f	0.331	0.224	0.091	0.312	0.166	0.182

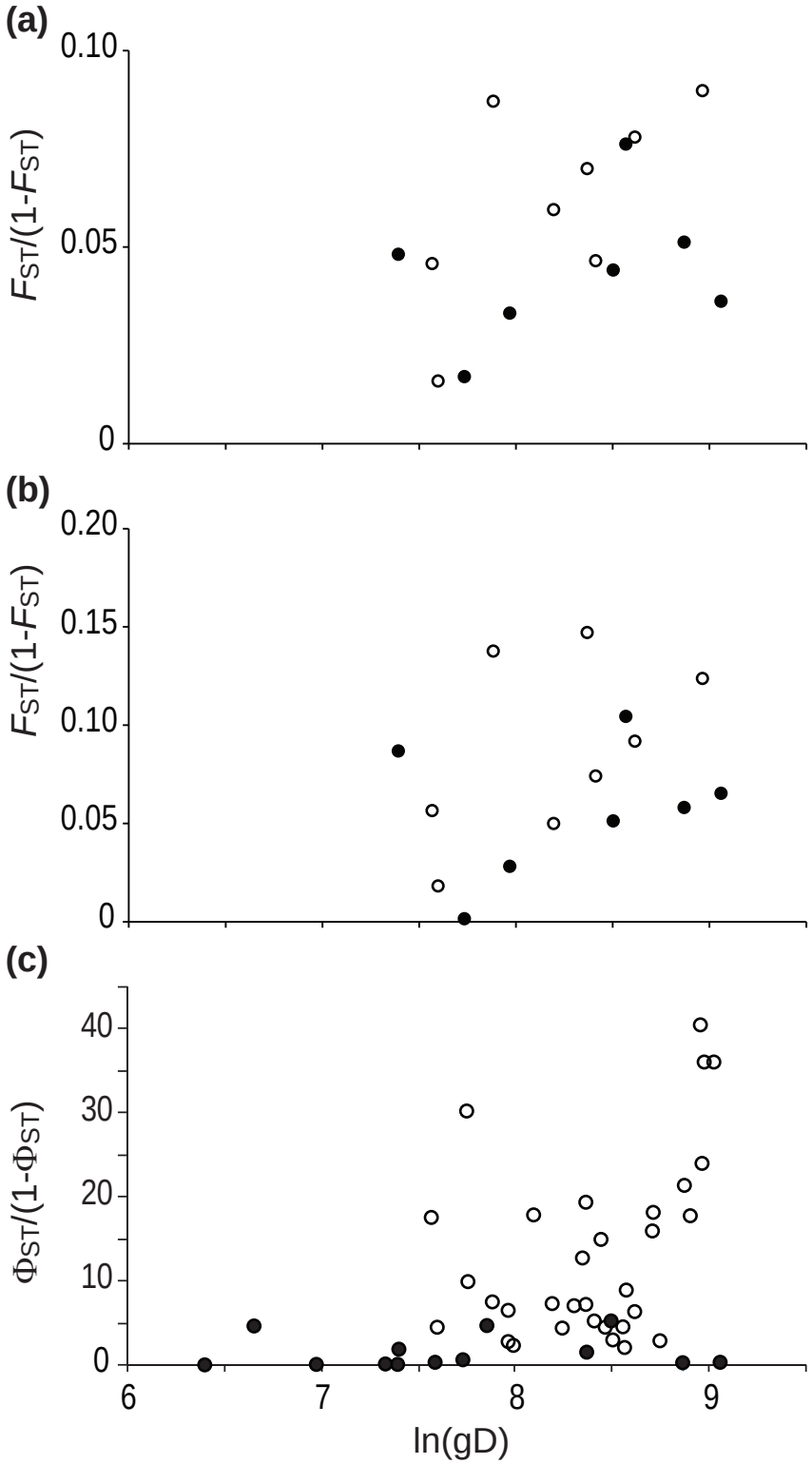

Online Resource 3 *Tridacna noae*. Pairwise estimates of genetic differentiation plotted against the logarithm of geographic distance [ln(gD), in km]. *Black circles* intra-lineage comparisons; *open circles* inter-lineage comparisons. Spatial pattern of genetic differentiation at nuclear loci estimated from genotypes at 6 **(a)** and 2 **(b)** microsatellite loci with correction for null alleles under FREENA (Chapuis and Estoup 2007). The Yap sample is considered as belonging to Lineage 1. Inter-lineage comparisons were generally higher than intra-lineage comparisons within the same range of geographic distances. Mantel test, 10 000 random permutations: $P = 0.177$ and $P = 0.124$ for (a) and (b), respectively. Spatial pattern of genetic differentiation at the mitochondrial locus **(c)** (the Yap sample being considered as belonging to Haplogroup I). Inter-lineage comparisons formed a cloud of points visibly distinct from intra-lineage comparisons within the same range of geographic distances. Mantel test, 10 000 random permutations: $P = 0.048$

Chapuis MP, Estoup A (2007) Microsatellite null alleles and estimation of population differentiation. Mol Biol Evol 24:621-631